Chemistry and Physics Faculty Articles

Department of Chemistry and Physics

Experimental and Modeling Studies of Secondary Organic Aerosol Formation and Some Applications to the Marine Boundary Layer

Song Gao
University of Washington - Seattle Campus, sg1002@nova.edu

Dean A. Hegg
University of Washington - Seattle Campus

Glendon Frick
Naval Research Laboratory

Peter F. Caffrey
Naval Research Laboratory

Louise Pasternack
Naval Research Laboratory

See next page for additional authors

Follow this and additional works at: https://nsuworks.nova.edu/cnso_chemphys_facarticles

Part of the Environmental Chemistry Commons

Authors

Song Gao, Dean A. Hegg, Glendon Frick, Peter F. Caffrey, Louise Pasternack, Chris Cantrell, William Sullivan, John Ambrusko, Thomas Albrechcinski, and Thomas W. Kirchstetter

Experimental and modeling studies of secondary organic aerosol formation and some applications to the marine boundary layer

Song Gao,[1] Dean A. Hegg,[1] Glendon Frick,[2] Peter F. Caffrey,[2] Louise Pasternack,[2] Chris Cantrell,[3] William Sullivan,[4] John Ambrusko,[4] Thomas Albrechcinski,[4] and Thomas W. Kirchstetter[5]

Abstract. A series of controlled experiments were carried out in the Calspan Corporation's 600 m^3 environmental chamber to study some secondary organic aerosol formation processes. Three precursor-ozone systems were studied: cyclopentene-ozone, cyclohexene-ozone, and α-pinene-ozone. Additionally, SO_2 was added to the initial gas mixture in several instances and was likely present at trace levels in the ostensibly organic-only experiments. It was found that all three systems readily formed new submicron aerosols at very low reactant levels. The chemical composition of formed aerosols was consistent with some previous studies, but the yields of organic products were found to be lower in the Calspan experiments. A three-step procedure is proposed to explain the observed particle nucleation behavior: HO· production → H_2SO_4 formation → H_2SO_4-H_2O (perhaps together with NH_3) homogeneous nucleation. It is also proposed that some soluble organic products would partition into the newly formed H_2SO_4-H_2O nuclei, enhance water condensation, and quickly grow these nuclei into a larger size range. While the observations in the two cycloolefin-ozone systems could be well explained by these proposed mechanisms, the exact nature of the nucleation process in the α-pinene-ozone system remains rather opaque and could be the result of nucleation involving certain organics. The results from three simple modeling studies further support these proposals. Their applicability to the marine boundary layer (MBL) is also discussed in some detail. Particularly, such a particle nucleation and growth process could play an important role in secondary aerosol formation and, quite likely, CCN formation as well in certain MBL regions.

1. Introduction

Organic aerosols have recently received immense attention as organic compounds have been found to be important constituents of atmospheric aerosols. It has been reported that total organic carbon can comprise 25-65% of the fine aerosol (diameter <2.5 micron) mass in local regions [*Wolff et al.*, 1991; *Chow et al.*, 1994; *Novakov et al.*, 1997]. In the marine boundary layer (MBL), according to the results from the First Aerosol Characterization Experiment (ACE 1), at least 10% of the marine aerosol mass is organic matter. In fact, organics and sulfate have been found to be often present in a single aerosol particle [*Murphy et al.*, 1998]. There have also been measurements showing that in both the polluted and background marine atmosphere, organic aerosols can play as important a role in cloud condensation nuclei (CCN) formation as sulfate aerosols [*Novakov and Penner*, 1993; *Matsumoto et*

al., 1997]. In addition, some laboratory studies have pointed out that aerosols composed of certain organic species as well as inorganic/organic mixtures have the ability to become CCN at typical atmospheric supersaturations [*Cruz and Pandis*, 1997, 1998; *Corrigan and Novakov*, 1999]. Because these organic compounds have quite different chemical, physical, hygroscopic, and optical properties from their inorganic counterparts, they could play significant and distinctive roles in aerosol and cloud-related processes, for example, affecting the direct and indirect aerosol climate forcing. However, despite their potential importance, there is still no complete inventory of organic compounds comprising fine aerosols due to their chemical complexity and the lack of appropriate analytical methods.

Among the known species, dicarboxylic acids (C2 ~ C10) are now recognized as ubiquitous components in the water-soluble portion of marine aerosols as well as polar and urban aerosols [*Grosjean et al.*, 1978; *Kawamura et al.*, 1996; *Kawamura and Sakaguchi*, 1999]. On average, these diacids can account for up to 16% of total organic aerosol mass in remote marine environments [*Kawamura and Sakaguchi*, 1999]. Some of the soluble diacids have been proven to be able to act as CCN at typical supersaturations in the MBL [e.g., *Corrigan and Novakov*, 1999]. Yet, not surprisingly, a lot of uncertainties still remain as to the atmospheric roles of these homologous compounds. One immediate concern is related to their secondary aerosol formation potential. It has long been postulated that dicarboxylic acids in the aerosols

[1]Department of Chemistry and Department of Atmospheric Sciences, University of Washington, Seattle, Washington.
[2]Naval Research Laboratory, Washington, D. C.
[3]National Center for Atmospheric Research, Boulder, Colorado.
[4]Calspan–University of Buffalo Research Center, Buffalo, New York.
[5]Lawrence Berkeley National Laboratory, Berkeley, California.

could be produced by in situ chemical oxidation of precursor compounds (anthropogenic and/or natural) followed by partitioning of the gaseous diacid products into the particulate phase [*Grosjean et al.*, 1978; *Satsumabayashi et al.*, 1990]. Reaction pathways of cycloolefins and ozone to produce diacids have been proposed in some detail through laboratory studies [*Hatakeyama et al.*, 1985, 1987; *Kalberer et al.*, 2000]. These smog chamber experiments showed particulate dicarboxylic acids were indeed formed from cycloolefin precursors. However, the concentrations of olefins and ozone that were used were often at least 4 to 5 orders of magnitude higher than the expected values in the MBL. In some other cases there were already seed particles present before the reactants were introduced into the chamber. Thus there is a need to explore if particulate diacids can be produced from precursors at ambient levels with no preexisting particles, and if so, how are these acids incorporated into the particulate phase (via homogeneous nucleation or other mechanisms)? Could sulfate and its formation be related to the organic aerosol formation process in some way? Additionally, what are the effects of such a process on aerosol and perhaps CCN formation in certain MBL regions where preexisting aerosols are at low concentrations (100~300 cm^{-3}) and cycloolefins could be present due to transport from the continent or other sources? These uncertainties also apply to many biogenic hydrocarbons which are emitted globally in large quantities and have considerable reactivity toward atmospheric oxidants [*Simpson et al.*, 1995; *Hoffmann et al.*, 1997]. For example, monoterpenes (α-pinene and analogous compounds), which are estimated to comprise 11% of volatile organic compounds emitted by vegetation [*Guenther et al.*, 1995], can be easily oxidized to produce condensable products exhibiting high aerosol yields. A number of smog chamber experiments and modeling efforts have been carried out to study monoterpene oxidation systems [*Odum et al.*, 1996; *Hoffmann et al.*, 1997, 1998; *Koch et al.*, 2000]. However, many results, while certainly of importance, are still highly speculative due to the complexity of the problem.

This work attempts to address the above specific uncertainties via controlled laboratory studies. We designed and carried out a series of experiments in the Calspan Corporation's environmental chamber to simulate some secondary organic aerosol formation processes and investigate the roles of organic products in particle formation, including comparisons with the better studied sulfates. Diagnostic modeling calculations were performed, prompted by some interesting experimental results. The applicability of these results to certain MBL regions is also discussed in this work.

2. Experimental Procedure

The Calspan Corporation's 600 m^3 chamber was carefully characterized in May 1998, when both physical and chemical measurements were made to test its functioning for chemical reaction and particle formation experiments. In addition, the concentration of background contaminants and wall loss of gases and particles in the clean chamber were determined. A more detailed description is given in a report on the characterization of the chamber [*Hoppel et al.*, 1999].

The main experiments were carried out in the characterized chamber in October and November of 1998. Three hydrocarbon precursor-ozone systems were studied: cyclopentene-

ozone, cyclohexene-ozone, and α-pinene-ozone. These three systems have been studied extensively but in most cases, either at precursor concentrations that are much higher than plausible values or in the presence of seed aerosol in the chamber [e.g., *Hatakeyama et al.*, 1985, 1987; *Hoffmann et al.*, 1997]. The fact that all these experiments have reported some sort of particle formation and the potential presence of these specific precursors (or related compounds) in certain regions of the atmosphere warrant another carefully designed laboratory study for our earlier-stated purposes. The experimental procedure was similar for all three systems, and is described as follows.

The chamber air was routinely filtered through charcoal and aerosol filters overnight to get a "clean" chamber. After such filtering, the mixing ratios of SO_2, NO_x, and O_3 were below detection limits of 0.1 ppbv, 0.5 ppbv, and 1 ppbv, respectively. The particle number concentration was always below 0.1 cm^{-3}. Then, for example, about 50 ppbv cyclopentene and 100 ppbv ozone were sequentially injected into this clean chamber and quickly mixed by a mixing fan. An air sample was drawn from the chamber at 15-min intervals and subsequently analyzed by a GC-MS to obtain the hydrocarbon precursor concentrations. The ozone concentration was continuously measured with a Dasibi Model 1008 ozone analyzer. The concentration of SO_2 was measured by a pulsed fluorescence SO_2 analyzer (Thermo Environmental Corp. Model 43S) continuously. A tunable diode laser absorption system (TDLAS) was employed to monitor the concentrations of NH_3 and H_2O_2 in the chamber. The NH_3 concentration was also monitored by a thermo oxidation NH_3 to NO_x converter (Dasibi Model 2109) coupled with a NO_x analyzer (Thermo Environmental Corp. Model 42) and compared with the measurements by TDLAS. The hydroxyl and peroxy radical concentrations were monitored by NCAR's chemical ionization mass spectrometer (CIMS). The particle number concentration in the chamber was measured by a TSI 3025A ($r > 3$ nm) and a TSI 3022 ($r > 10$ nm) particle counter simultaneously (at 90% counting efficiency). A differential mobility analyzer (DMA) from Naval Research Laboratory (NRL) was used to obtain the particle size distribution (threshold $r > 5$ nm), from which calculated values of the particle volume density and surface area were derived. The chamber temperature, pressure, and relative humidity were monitored by respective NRL instruments. Such an experiment was repeated and/or carried out under slightly different conditions, for example, at a different RH or with a different amount of added SO_2 or NH_3, to examine their effects on particle formation. It is worth noting that since the DMA actually measures dry aerosol properties, the measured aerosol size and volume should be corrected to obtain the actual values in the more humid chamber. However, since most of our discussions in the next section are based on comparisons of a set of measurements at a similar RH, such a correction can be ignored in these cases. We will, on the other hand, perform such hygroscopic corrections in the "Partitioning of glutaric acid into the fresh H_2SO_4-H_2O nuclei" modeling calculations.

The aerosols produced, if any, were collected onto a dual tandem filter arrangement (Teflon filter followed by quartz filter in one path, tandem quartz filters in another parallel path) connected to the chamber through the wall [*Turpin et al.*, 1994]. Each Teflon filter was then dissolved in 10 mL deionized water, and the extract was analyzed by a DIONEX DX500

Table 1. Particle Nucleation in O_3-Only Chamber and Three Hydrocarbon-O_3 Systems

Cases	Clean Chamber With 100 ppbv Ozone (Dark) (Oct. 10, 1998)	Clean Chamber With 50 ppbv Cyclopentene and 100 ppbv Ozone (Nov. 10, 1998)	Clean Chamber With 60 ppbv Cyclohexene and 135 ppbv Ozone (Oct 16, 1998)	Clean Chamber With 16 ppbv α-Pinene and 95 ppbv Ozone (Nov. 9, 1998)
T, °C	25	26	25	25
RH, %	33	29	49	29
N_m,[a] cm^{-3}	20	2.6 K	2.5 K	20 K
R_m,[b] nm	<5	32	35	30
V_p,[c] μm^3 cm^{-3}	0.02	0.40	0.87	1.21

[a] N_m is maximum particle number concentration.
[b] R_m is mean particle radius at the end of particle growth.
[c] V_p is particle volume density after a certain time of growth (see text)

ion chromatography system to identify water-soluble compounds in the aerosols. The quartz filters were analyzed with an evolved gas analysis (EGA) method at the Lawrence Berkeley National Laboratory for total carbon (TC) mass. This method has been described in detail in several recent publications [e.g., *Novakov et al.*, 1997]. The dual tandem filter arrangement was used to correct the estimates of aerosol carbon mass for the possible adsorption of organic vapors onto the quartz filters.

3. Results and Discussions

3.1. Particle Nucleation in the Hydrocarbon-Ozone Systems

In all three hydrocarbon-ozone systems, new submicron particles were formed at low precursor levels, as is shown in Table 1. In the case of November 10 the particle number concentration in the chamber was below 10 particles/cm³ before 50 ppb of cyclopentene and 100 ppb of ozone were injected into the chamber. Within 3 min after injections, ultrafine particles started to be detected by the TSI 3025A particle counter (r > 1.5 nm, at 50% counting efficiency). The DMA started to detect particles (r > 5 nm) and measure their size distribution within 10 min after the nucleation onset. The particle number concentration increased steadily and reached a maximum of 2600 cm⁻³ (N_m) in about 30 min. In the meantime the mean radius of the formed particles reached a maximum of 32 nm (R_m), while the volume density (V_p) reached 0.40 μm³/cm³. Qualitatively, similar behaviors were observed in the cyclohexene-ozone system and α-pinene-ozone system (Table 1) where new submicron particles were formed.

In contrast, when 100 ppb ozone alone was injected into the clean chamber on October 10, almost no new particles were formed in the next hour of observation. The measured particle concentration was always below 20 cm⁻³. During the 30 min from the nucleation onset, the mean radius of particles never exceeded 5 nm (not detected by the DMA), and the particle volume density was always below 0.02 μm³/cm³. The much smaller R_m and V_p here are in sharp contrast with those in the hydrocarbon-ozone experiments as shown in Table 1. Clearly, the oxidation products of these organic precursors significantly contributed to the new submicron particle production in the chamber. While such a particle formation behavior in the cycloolefin-ozone and monoterpene-ozone systems has been reported in some earlier smog chamber

studies [*Hatakeyama et al.*, 1985, 1987, 1989], the concentrations of the hydrocarbon precursors they used were much higher (up to 3 orders of magnitude). Our results show that at mixing ratios of tens of ppbv, much closer to the possible values in the MBL [*Grosjean et al.*, 1978; *Bonsang et al.*, 1991], these cycloolefins and monoterpenes can readily form new submicron particles in the presence of ozone.

We note the average concentrations of cycloolefins in the MBL are possibly even lower than in this study. However, in some MBL regions such as those near urban centers, cycloolefins could potentially reach ppbv levels due to offshore transport under certain conditions. Therefore our results in this study can be directly applicable to such MBL regions where hydrocarbon precursor concentrations are somewhat elevated.

3.2. Chemical Analyses of Formed Aerosol

It is important to know what chemical species in these precursor-ozone reaction systems were produced and incorporated into the particulate phase. The initial conditions as well as the mass concentrations and molar yields of particulate products identified by ion chromatography (IC) are listed in Table 2. The carbon-based molar yield of a product (in the aerosol), which indicates the percentage of the reactant converted into this product, is defined by [Δproduct (mol) × carbon number of the product / (Δhydrocarbon (mol) × carbon number of the hydrocarbon)] × 100. The molecular structures of the three hydrocarbon precursors, selected oxidation products and a possible reaction intermediate (Criegee intermediate) are listed in Table 3.

The three cyclopentene (CP)-ozone cases show that glutaric acid was the most abundant particulate product identified by IC, followed by succinic acid. The ratio of C5 to C4 diacid yield was about 6 in all three CP-O_3 cases, which implies a stable reaction mechanism for dicarboxylic acid productions with distinct branching ratios could exist. However, this awaits further investigation. Comparing the total diacid mass concentration (from IC) with the aerosol volume concentration measured by DMA, if we assume an aerosol mass density of 1 g/cm³, dicarboxylic acids constitute about 15% of the total aerosol mass, which is consistent with earlier findings [*Hatakeyama et al.*, 1987]. This also consistently shows secondary aerosol components in the CP-O_3 system could include other oxidation products, predominantly dialdehydes and ω-oxo carboxylic acids. The most abundant aerosol components in the cyclohexene-ozone case, identified by IC,

Table 2. Initial Conditions, Chemical Composition, and Molar Yields of Products in Selected Hydrocarbon-Ozone Experiments[a]

Hydrocarbon	Cases	$[HC]_o$, ppb	$[O_3]_o$, ppb	T, °C/RH, %	$\Delta[HC]$, ppb	Mass Concentration of Identified Species, $\mu g\ m^{-3}$	Carbon-Based Molar Yield, %	Molar Yield (%) of Total Dicarboxylic Acids
Cyclopentene	Oct. 10	50	100	27/66	46	glutarate 0.41 succinate 0.09	GA 0 17 SA 0.03	0.20
	Nov. 14 before noon	50	90	24/68	39	glutarate 0.27 succinate 0.05	GA 0.13 SA 0.02	0.15
	Nov. 14 after noon	50 $[SO_2] = 1$ ppb	100	24/70	50	glutarate 0.57 succinate 0.15 sulfate 0.08;	GA 0.23 SA 0.05 SF[b] 2	0.28
Cyclohexene	Oct. 16	60	150	25/43	36	adipate 0.30 glutarate 0.30 succinate 0.03	AA[c] 0.14 GA 0.13 SA 0.01	0.28
α-pinene	Oct. 19	20	115	26/48	13	TC 2.37	3.7 (carbon)	N/A
	Nov. 9	16	95	25/29	16	TC 2.98	3.8 (carbon)	N/A

[a] $[HC]_o$ is the initial mixing ratio of hydrocarbon, $[O_3]_o$ is the initial mixing ratio of ozone, T (°C) is the temperature in the chamber, RH (%) is the relative humidity in the chamber, $\Delta[HC]$ is the hydrocarbon consumed during the 40-min period; mass concentration is that of each organic product identified by the IC. GA, glutaric acid; SA, succinic acid; AA, adipic acid; SF, sulfuric acid; TC, total carbon; N/A, not available.

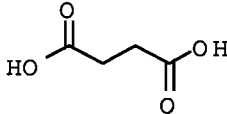[b] The molar yield of SF is calculated based on sulfur moles, not carbon moles.
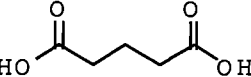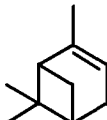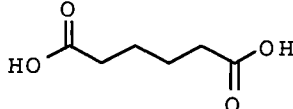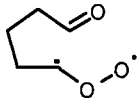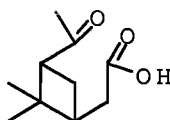
[c] Tentatively identified as AA. It could also be one of its isomers, e.g., a hydroxy-ketoacid.

were adipic acid (tentatively) and glutaric acid, with a very minor product being succinic acid.

It is useful to note here that ion chromatography turns out to be very suitable for the detection of dicarboxylic acids, which are highly polar and water-soluble compounds. Theoretically, those hydrocarbon oxidation products with carbons at the highest oxidation state (e.g., diacids) should be the least volatile and most water-soluble among all the products. Thus, for the purpose of studying particle nucleation, we have chosen to use IC instead of the more widely used GC-MS or GC techniques which often have difficulty in identifying polar compounds without prior derivatization [e.g., Yu et al., 1999]. The detection limits of the IC for adipic, glutaric and succinic acids were 0.04, 0.04, and 0.01 $\mu g/m^3$, respectively (at a

Table 3. Molecular Structures of Hydrocarbon (HC) Precursors, a Possible Reaction Intermediate, and Selected Oxidation Products

HC Precursor (and a Possible Reaction Intermediate)	Molecular Structure	Selected Oxidation Product	Molecular Structure
Cyclopentene		succinic acid	
Cyclohexene		glutaric acid	
α-pinene		adipic acid	
Criegee intermediate (in cyclopentene-ozone system)[a]		pinonic acid[b]	

[a] A possible reaction intermediate in the cyclopentene-ozone reaction system. Criegee intermediates in other precursor-ozone systems are analogous to this one in structure.

[b] One of the identified ozonolysis products of α-pinene.

typical sampling volume of 4 m^3). The overall uncertainty for measured diacid concentrations was about ±20%. With NaOH as the eluent and a gradient elution method, each diacid eluted at a specific elution time that was determined by running a standard compound under the same IC condition. The separation of those consecutively eluted diacids was reasonably good. For example, the resolution between the adjacent glutarate and succinate peaks was, on average, 80%.

It is interesting to note that the carbon-based molar yields of total diacids in aerosols are quite a bit lower in our experiments (~0.2% in CP-O$_3$ case; ~0.3% in CH-O$_3$ case) than in those carried out by *Hatakeyama et al.* [1985, 1987] (~0.6% in CP-O$_3$ case; ~6%, in CH-O$_3$ case). Such comparisons are made with regard to the yields after about the same reaction time. As discussed in more detail later, this yield difference could be due to the fact that the initial ozone (and cycloolefin) concentrations in those earlier experiments were at least 3 orders of magnitude higher than in the experiments reported here. The lower initial concentrations led to smaller amounts of organic products in the gas phase which, due to the resultant lower driving force, partitioned into the particulate phase at much smaller amounts.

It is also worth noting that the above mass concentrations and yields, in most cases, are based upon the measurements of aerosol samples collected during a 40-min interval, usually starting ½ hour from the nucleation onset. However, previous studies suggest that if the formed aerosols were given enough time to evolve in the chamber (e.g., 24 hours), dicarboxylic acids could actually comprise more than 50% (mass) of the total secondary aerosol products [e.g., *Hatakeyama et al.*, 1987]. Earlier experimental data strongly suggest a sequential oxidation mechanism, in which further oxidations of some intermediate products to diacids could slowly take place on the aerosol surface or in the gas phase. Because of the shortage of time, we were not able to collect aerosols after such a long time (24 hours). However, it should be kept in mind that in the ambient atmosphere, where enough time is often available, the dicarboxylic acids can have much higher aerosol yields than those shown in Table 2. These diacids can therefore comprise a major mass fraction of the secondary aerosols formed in similar cycloolefin-ozone systems. This provides an important basis for our later modeling calculations.

The mass concentrations of total organic carbon in the collected aerosols in the October 10, October 16, and November 14 after noon cases were 6 μgC/m^3, 1.01 μgC/m^3, and 1.26 μgC/m^3, respectively, according to the EGA results. The total aerosol mass concentrations, derived from the DMA measurements, were 5.3 μg/m^3, 3.62 μg/m^3, and 4.82 μg/m^3, respectively, in the above three cases, assuming a unit density of the aerosol. However, it is quite difficult to compare these two sets of measurements in a straightforward manner due to at least two uncertainties: the uncertainty of the aerosol density and the uncertainty of the average molecular weight of aerosol organic matter. The sampling artifacts of the EGA method could further add to the difficulty of any direct comparison [*Huebert and Charlson*, 2000]. Nevertheless, these measured organic carbon concentrations and total aerosol mass concentrations support our contention that secondary aerosols are indeed formed in the cycloolefin-ozone systems under atmospheric conditions and they contain a large fraction of organic matter.

Table 4. Nucleation and Growth Behaviors of H$_2$SO$_4$ and Cyclopentene-Ozone Products

Injected Gaseous Precursors	October 10, 1998 150 ppbv Ozone	October 13, 1998 150 ppbv Ozone; 10 ppbv SO$_2$	November 10, 1998 100 ppbv Ozone; 50 ppbv Cyclopentene
T, °C	25	24	26
RH, %	33	35	29
J_n,[a] cm^{-3} s^{-1}	~0	350	3.0
N_m,[b] cm^{-3}	20	over 100 K	2.6 K
R_m,[b] nm	<5	~5	32
V_p,[b] μm^3 cm^{-3}	0.02	0.003	0.43

[a]J_n is particle nucleation rate derived from particle counter measurements.

[b]These notations are identical to those used in Table 1.

In several previous studies, secondary aerosol formation from reaction of α-pinene with O$_3$ has been observed and a series of oxidation products have been identified, some of which are suspected to play important roles in new particle formation [*Hatakeyama et al.*, 1989; *Hoffmann et al.*, 1998]. However, no organic product was detected by the IC in the aerosol samples collected in the α-pinene-ozone experiments in the Calspan chamber. In contrast, the EGA results showed high yields of particulate carbon (~4% yield), as shown in Table 2. These results strongly suggest at the low reactant levels used in the Calspan chamber, low-volatility, rather insoluble and/or nonpolar products were produced and incorporated into the particulate phase. However, the chemical nature of these oxidation products still awaits further elucidation despite some recent attempts [e.g., *Yu et al.*, 1999].

3.3. Nucleation and Growth Behaviors of H$_2$SO$_4$ and Organic Products

In Table 4 the average time derivative of particle number concentrations, measured by TSI 3025A particle counter, is calculated as an indication of the particle nucleation rate J_n. When only ozone was in the chamber (October 10, 1998), the particle nucleation rate was negligible (~0). When SO$_2$ or cyclopentene was added into the chamber, J_n was enhanced. However, at similar T and RH, the enhancement of J_n in the SO$_2$-O$_3$ case was 2 orders of magnitude greater than in the cyclopentene-ozone case. Also, far higher maximum particle concentration was observed in the SO$_2$-O$_3$ case as seen from the differences of N_m. These particles were very small (mean radius R_m ~ 5 nm) during the 40-min observation period and had a very low volume density (V_p ~ 0.003 μg/m^3), in contrast to the much larger particles (but less in number concentration) eventually formed in the cyclopentene-ozone system. Such a contrast was also observed in other SO$_2$-O$_3$ and cyclopentene-ozone cases. In addition, cyclohexene-ozone exhibited a similar behavior to the cyclopentene-ozone system. These results clearly indicate SO$_2$-O$_3$ system has a much greater particle nucleation potential than cycloolefin-ozone system whereas the latter produced much larger particles. The α-pinene-ozone system is somewhat different than the two cycloolefin-ozone systems: while particles also grew to a similarly large size eventually (R_m ~ 30 nm, Table 1), far more particles were formed in the meantime. In fact, the particle number concentration in the α-pinene-ozone case was found to be usually higher than the cycloolefin-ozone case, but lower

than the SO_2-O_3 case, when the precursor concentrations were comparable (e.g., see Tables 1 and 4).

Perhaps the most interesting fact here is that in the October 13 case, a huge number of tiny particles were produced in the SO_2-O_3 system. Such a behavior agrees with the much studied behavior of H_2SO_4-H_2O homogeneous nucleation. Indeed, H_2SO_4 is the only common species that has a low enough vapor pressure to nucleate new particles at such a high rate. On the other hand, it is well known that, in the gas phase (dark condition, no ozone photolysis), SO_2 and O_3 would react to produce H_2SO_4 only at an extremely slow rate. Reaction with HO· is the dominant oxidation process of SO_2 [Stockwell and Calvert, 1983]. Hence the following pathway is proposed to interpret the observed particle formation in SO_2-O_3 cases:

In the dark chamber, particle production was in fact due to H_2SO_4-H_2O homogeneous nucleation. Hydroxyl, the needed oxidant for SO_2, was produced from the oxidation of background hydrocarbons rather than ozone photolysis. The characterization of the "clean" chamber showed that low though significant amounts of hydrocarbons were in the overnight filtered chamber. For example, a few ppbv haloalkanes and aromatic compounds were detected by a GC-MS [Hoppel et al., 1999]. This suggests that more reactive hydrocarbons such as alkenes (for which no specific analysis was made, i.e., no standards were run) could also have been present. These hydrocarbons could have reacted with the injected O_3 to produce Criegee intermediates and HO·, the latter often being produced with a high yield [Atkinson, 1994]. Then either the Criegee intermediate or HO· could easily oxidize the injected SO_2 to produce H_2SO_4 followed by particle nucleation. Calculations indicate the Criegee intermediates would react quickly with water vapor in the chamber or go through other oxidation processes, leaving HO· as the most possible oxidant for SO_2 oxidation. The validity of such a pathway is further supported by the observed HO· production detected by the CIMS after ozone was injected into the "clean" chamber. In all the cases where 30 ppbv or more of ozone was injected, CIMS immediately detected the production of HO· at up to 20 pptv in mixing ratio. The recent hypothesis of stable sulfate clusters (1-3 nm in diameter) serving as a source of new atmospheric particles [Kulmala et al., 2000], based on theoretical calculations and model simulations, is quite consistent with our proposal stated above. To better understand the particle formation process in the cyclopentene-ozone case, and in hydrocarbon-ozone cases in general, we carried out two further experiments as described below.

3.4. Impact of SO_2 on Particle Formation in Hydrocarbon-Ozone Systems

In the four cases listed in Table 5, similar amounts of α-pinene and O_3 were added into the chamber. In fact, $[O_3] \times [\alpha$-pinene] varied by less than 10%, which means the production rate and amount of organic compounds would vary within 10%. Different amounts of SO_2 were added into the chamber between α-pinene and ozone injections. The small amounts of added SO_2 should not affect the ozone amount (thus the oxidation of α-pinene) in the four cases by more than 6%. However, we see significant variations in the particle formation behavior (e.g., at least by a factor of 2 for J_n), presumably attributable to the added SO_2. When more SO_2 was in the chamber before the nucleation onset, the nucleation rate J_n turned out to be faster; more particles (larger N_m) were formed,

Table 5. Impact of SO_2 on α-Pinene-Ozone Particle Formation

	Nov. 9, 1998	Nov. 18, 1998	Nov. 12, 1998	Nov. 11, 1998
[Ozone],[a] ppbv	95	110	110	100
[α-pinene],[b] ppbv	16	15	15	15
[Ozone]* [α-pinene]	1520	1650	1650	1500
T, °C	25	25	24	25
RH, %	29	30	43	47
[SO_2],[c] ppbv	trace (<0.1)	0.5	2.5	6
J_n,[d] $cm^{-3} s^{-1}$	22.2	174.7	779.2	1621 6
N_m,[d,e] cm^{-3}	14 K	73 K	187 K	380 K
R_m,[d] nm	32	not available	16	12

[a][Ozone] is ozone mixing ratio.
[b]Here [α-pinene] is α-pinene mixing ratio.
[c][SO_2] is SO_2 mixing ratio.
[d]These notations are identical to those used in Table 4.
[e]These are measurements from the CN3022 particle counter which efficiently counts particles larger than 10 nm in radius. The CN3025A counter has a dynamic range extending only to 100 K cm^{-3}.

and the mean size of the particles (R_m) showed a decreasing trend. Such an impact of SO_2 on particle formation was also observed in the cyclopentene-ozone system and cyclohexene-ozone system. These results show that in these hydrocarbon-ozone systems, even a few ppb of SO_2, if present, would play a crucial role in nucleating new particles. Furthermore, our model calculations, described in detail in section 4.1, suggest the gaseous organic products in these two cycoolefin-ozone systems do not readily form new particles through homogeneous nucleation. Therefore it is reasonable to believe that trace amounts of H_2SO_4 (from SO_2 oxidation) initiated particle nucleation in the cycloolefin-ozone cases where SO_2 could certainly have been present at trace levels (<0.1 ppbv). In the α-pinene-ozone cases (e.g., November 9, Table 5), more particles were formed than in the cycloolefin-ozone cases (e.g., November 10, Table 4) under similar T and RH. We have shown earlier that high yields of organic products (carbon) were found in the aerosols in the α-pinene-ozone system (Table 2). The possibility then exists that some organic products in this particular system contributed to new particle formation through homogeneous nucleation. However, the huge particle nucleation potential of H_2SO_4 as shown in Tables 5 and 4 also suggests that sulfuric acid could still be the major nucleating species even in the α-pinene-ozone system. On the other hand, it is again evident (R_m in Tables 5, 4, and 1) that oxidation products of hydrocarbon precursors grew the fresh nuclei into a much larger size range than in the SO_2-O_3 system.

3.5. Impact of Water Vapor Partial Pressure on Hydrocarbon-Ozone Particle Formation

In the case of the cyclopentene-ozone system the relative humidity was changed to study the impact of water vapor partial pressure P_w^0 on particle formation. The results, listed in Table 6, indicate that a higher P_w^0 produced more particles (larger N_m) and increased the nucleation rate J_n. When we consider the binary nucleation rate equation: $J = 4 \pi r^2 N_1 \beta_2 \exp[-\Delta G/(kT)]$, where N_1 is water molecule (component 1) concentration and β_2 is the impingement rate of another nucleating species (component 2), it is conceivable that the nucleation we observed was quite possibly a binary (or even ternary) nucleation system with water as one nucleating species. As we have mentioned in section 3.4 and will further show with some modeling calculations, such a nucleating system is most

Table 6. Impact of Water Vapor Partial Pressure on Cyclopentene-O_3 Particle Formation

	October 10, 1998	November 14, 1998 (Before Noon)	November 10, 1998
[Cyclopentene],[a] ppbv	50	50	50
[Ozone],[b] ppbv	100	90	100
T, °C/RH, %	27/66	23/64	26/29
Pw^{o},[c] Pa	2400	1800	980
J_n,[d] cm^{-3} s^{-1}	81.5	37.2	3.0
N_m,[d] cm^{-3}	24 K	14 K	2.6 K
R_m,[d] nm	37	40	32
V_p,[d] μm^3 cm^{-3}	5.3	3.7	0.54
Mass concentration of products, μg m^{-3}	glutarate 0.41; succinate 0.09;	glutarate 0.27; succinate 0.05;	below detection limit of IC

[a][Cyclopentene] is cyclopentene mixing ratio.
[b][Ozone] is ozone mixing ratio.
[c]Pw^{o} is water vapor partial pressure.
[d]These notations are identical to those used in Table 4.

likely H_2SO_4-H_2O in the ostensibly cycloolefin-ozone case. Analogous to the pathway we proposed earlier in section 3.3, the following (a)-(b)-(c) three-step procedure would produce fresh H_2SO_4-H_2O nuclei:

Even though SO_2 was below the detection limit of the SO_2 analyzer, trace amounts (i.e., lower than 0.1 ppbv) were very likely present that could be quickly oxidized to produce H_2SO_4. In fact, in the case of November 14 before noon (Table 6), 1~2 ppt of H_2SO_4 vapor was detected by the CIMS during the 20-min period after cyclopentene and ozone were injected into the chamber. Considering also the likely presence of NH_3 (a few pptv at least) as a contaminant, such a H_2SO_4-H_2O-NH_3 ternary system constitutes one of the best known systems exhibiting a high nucleation potential [Coffman and Hegg, 1995]. Additionally, as we can see from Table 2, glutaric acid (GA), succinic acid (SA), and other organic products were produced in much larger quantities than if no cyclopentene was injected. A possible reaction pathway from cyclopentene to its oxidation products is through the formation of a Criegee intermediate and its further oxidation, as depicted above. Considering their low volatility (compared with other gaseous products, e.g., formic acid) and appreciable water solubility, these diacids are expected to partition into the fresh H_2SO_4-H_2O nuclei, initiate substantial water condensation and quickly grow the particles into a larger size range (~30 nm). Such a scheme could well explain many of our observations, for example:

1. In the SO_2-O_3 case (Table 4, October 13) the oxidation products from background hydrocarbons alone did not provide enough mass (to initiate substantial water condensation), thus never grew the nuclei big enough to be detected by the DMA (R_m always below 5 nm during the 40-min observation period).

2. In the O_3-only case (Table 4, October 10) the lack of hydrocarbon precursors yielded very little hydroxyl so that, with possibly only a trace amount of SO_2 in the chamber, very

little H_2SO_4 was produced, and essentially no particle production was observed.

3. In the cases listed in Table 5, with similar amounts of organic species (and water) for partitioning, the mean particle size decreased as the initial SO_2 mixing ratio increased, since more H_2SO_4-H_2O fresh nuclei would be formed at the higher SO_2 levels and share the available partitioning species.

4. When SO_2 was deliberately added into the chamber with hydrocarbon and ozone (e.g., November 14 after noon case in Table 2), sulfate was detected in the collected aerosol samples due to the relatively large mass of produced H_2SO_4. When no SO_2 was injected (so that its concentration was below the detection limit of 0.1 ppbv), the mass of H_2SO_4 produced was so low that no particulate sulfate was detected by the IC (e.g., October 10, November 14 before noon, and October 16 cases in Table 2). On the other hand, the organic species detected in the latter three cases indicated they, rather than sulfate, were the major contributors to the particle growth.

5. It is worth noting that the α-pinene system could be an exception to this proposed scheme. The ozone oxidation products of α-pinene could have very low volatility due to the rigid ring structure and large carbon numbers in the molecule. Therefore some of these products could directly participate in the homogeneous nucleation to from new particles [Hoffmann et al., 1998; Koch et al., 2000]. However, as indicated by the same authors, this hypothesis is still highly speculative both experimentally and theoretically. As we have shown in Table 5, just a few ppbv SO_2 would dramatically increase the nucleation rate and new particle number concentration. It seems for many moderately polluted conditions (particularly the MBL), where SO_2 is ubiquitous and terpenes rather rare (except when there are sufficient biogenic emissions), nucleation of H_2SO_4-H_2O is more likely.

3.6. Impact of Ammonia on Hydrocarbon-Ozone Particle Formation

It has been suggested [Coffman and Hegg, 1995; Korhonen et al., 1999] that ammonia could greatly enhance the binary nucleation rate J_n of the H_2SO_4-H_2O system. For example, the modeling results of Coffman and Hegg [1995] show when the H_2SO_4 mixing ratio is 2 pptv, just 1 to 5 pptv of NH_3 would enhance the J_n by 5 to 11 orders of magnitude, respectively. It

Table 7. Effect of Ammonia on α-Pinene-Ozone Particle Formation

Date (1998)	[α-pinene],[a] ppbv	[Ozone],[b] ppbv	T, °C/RH, %	[NH$_3$],[c] ppbv	J_n,[d] cm^{-3} s^{-1}	N_m,[d] cm^{-3}	R_m,[d] nm	V_p,[d] μm^3 cm^{-3}
Nov. 9	16	95	25/29	1.5 (upper limit)	23	20 K	32	1.75
Nov. 10	15	100	25/29	22.6	44	30 K	28	1.63

[a]Here [α-pinene] is α-pinene mixing ratio.
[b][Ozone] is ozone mixing ratio.
[c][NH$_3$] is NH$_3$ mixing ratio.
[d]These notations are identical to those used in Table 4.

therefore seems necessary to explore whether ammonia has any such effect on particle formation in the hydrocarbon-ozone systems studied in the Calspan chamber. In the following two cases listed in Table 7, different amounts of NH$_3$ were initially present in the chamber, with α-pinene and ozone, before the nucleation onset.

Clearly, the change of ammonia mixing ratio had only a very minor effect (less than a factor of 2) on either particle nucleation rate J_n, maximum particle number concentration N_m, mean particle size at the end of growth R_m, or particle volume density 40 min after the nucleation onset V_p. In the cases of cyclopentene-ozone and cyclohexene-ozone, our observations also showed a very minor impact of ammonia on new particle formation. This is hardly surprising if we note that, while there was possibly a trace amount of H$_2$SO$_4$ in the chamber (<5 pptv in most cases, according to the CIMS measurements), the ppbv level of NH$_3$ in the chamber (as a contaminant) should have almost certainly saturated the H$_2$SO$_4$. As a result, the enhanced nucleation rate was already included in the J_n of the November 9 case. More NH$_3$ would not further enhance the J_n such as in the November 10 case. In fact, this is quite consistent with the recent modeling work by *Korhonen et al.* [1999] which does suggest such an "insensitivity" of the nucleation rate to additional NH$_3$ beyond a rather low threshold. We note the observed small differences in J_n or N_m could be easily due to measurement errors.

Similarly, as shown by Table 7 (specifically, R_m and V_p), the rate and/or amount of organic products and water, which partitioned into the fresh nuclei and contributed to the aerosol growth, were neither significantly affected by ammonia. The intrinsic reason here is because almost all of the acidic products (e.g., dicarboxylic acids, pinonic acid) are weak acids (e.g., for glutaric acid, $pK_a^1 = 4.31$ at 298 K), therefore showing little chemical reactivity toward a weak base like NH$_3$·H$_2$O ($pK_b = 4.75$ at 298 K). Thus the partitioning of these species into the fresh nuclei should not be effectively enhanced by NH$_3$. For this same intrinsic reason, we further note, NH$_3$ is also not expected to enhance the nucleation rate of the systems that might include certain organic species such as some α-pinene oxidation products (if they had low enough vapor pressures for homogeneous nucleation). In addition, ozonolysis products of cycloolefins and α-pinene other than diacids, e.g., dialdehydes and ω-oxo carboxylic acids, should also not be affected by added NH$_3$ in terms of their nucleating abilities. Their molecular structures simply render them such weak acids that no considerable decrease in their vapor pressures can occur due to added NH$_3$.

4. Modeling Studies of Particle Nucleation and Growth

We have proposed that when cycloolefin and ozone were present in the chamber, and their reaction products were incorporated into secondary aerosols, the actual particle formation process was homogeneous nucleation of H$_2$SO$_4$ and H$_2$O (and perhaps NH$_3$), followed by partitioning of the organic products and water into the fresh nuclei. The H$_2$SO$_4$ was produced by the oxidation of trace amounts of SO$_2$ likely present in the chamber, whereas the partitioning of organic compounds into the nuclei was essentially due to their water solubility. Three simple modeling studies will further show why we believe these proposals are valid and also lead to some applications of these findings to secondary aerosol formation in the MBL.

4.1. Feasibility of Glutaric Acid-Water Binary Nucleation in Forming New Particles

As is shown in Table 2, glutaric acid (GA) is one of the major water-soluble species in the aerosol produced in the cyclopentene-ozone system, constituting more than 80% (mass) of aerosol components detected by ion chromatography. Meanwhile, GA is expected to have the highest particle nucleation potential considering its vapor pressure is the lowest among all the known products [*Hatakeyama et al.,* 1987]. Known reaction mechanisms [e.g., *Koch et al.,* 2000] actually suggest that GA, with two carboxyl groups in its molecular structure (and thus a high potential to form hydrogen bonds), is presumably the least volatile among the possible ozonolysis products of cyclopentene. It thus becomes important to evaluate if GA could indeed be the major nucleating species. We will study the feasibility of GA-H$_2$O nucleation by applying the classical binary nucleation theory [e.g., *Kiang et al.,* 1973]. For our purpose, both hydrate formation and the Zeldovich nonequilibrium factor are neglected.

The model maps out a free energy surface based on the values of ΔG defined by

$$\Delta G = -n_1 kT \ln\left(\frac{S_1}{a_1}\right) - n_2 kT \ln\left(\frac{S_2}{a_2}\right) + 4\pi r^2 \sigma, \qquad (1)$$

where k is the Boltzmann constant, T is the temperature, S_i is the saturation ratio of component i in the gas phase, a_i is the activity of component i in cluster solution, r is the radius of a cluster containing n_1 molecules of H$_2$O and n_2 molecules of GA, and σ is the surface tension of the cluster. By definition, we have

$$S_i = \frac{P_i}{P_{i,\text{eqm}}}, \quad a_i = \frac{P_i^{\infty}}{P_{i,\text{eqm}}}, \tag{2}$$

where P_i is the ambient vapor pressure of component i, $P_{i,\text{eqm}}$ is the equilibrium vapor pressure of pure component i, and P_i^{∞} is the equilibrium vapor pressure of component i over a flat surface of the binary solution with the same composition as the cluster.

ΔG in (1) is the free energy required to form a cluster of composition $(n_1 + n_2)$. At the saddle point of this free energy surface, the system is minimized. The nucleation rate can then be calculated by multiplying the steady state population of critical clusters by an "impingement rate" of the GA molecules (assumed far less than H_2O molecules in number concentration):

$$J = 4\pi r^2 \beta_2 N_1 \exp\left(\frac{-\Delta G^*}{kT}\right), \tag{3}$$

where N_1 is the number concentration of water vapor molecules, β_2 is the impingement rate of GA molecules onto critical clusters, $\beta_2 = N_2 (k T/(2 \pi M_2))^{1/2}$, M_2 is the mass of one GA molecule, and ΔG^* is the free energy at the saddle point.

The saddle point can be determined by solving

$$\left(\frac{\partial \Delta G}{\partial n_i}\right)_{n_j} = 0 (i, j = 1, 2, i \neq j), \tag{4}$$

which can also be written as

$$\ln\left(\frac{S_i}{a_i}\right) = \frac{2}{kT}\frac{M_i}{\rho}\frac{\sigma}{r}\left[1 - \frac{100 - X_i}{\rho}\frac{d\rho}{dX_i}\right], \tag{5}$$

where ρ is the density of the cluster at the binary composition, M_i is the mass of one molecule of component i, and X_i is the weight percentage of component i in the cluster which is defined as

$$X_i = \frac{100 n_i M_i}{n_1 M_1 + n_2 M_2}. \tag{6}$$

Equation (5) omits the surface tension derivative term $(d\sigma/dX_i)$, as in the work of Renninger et al. [1981] and Wilemski [1984].

At this point, we introduce the following expressions:

$$\rho = \frac{\rho_1 n_1 M_1 + \rho_2 n_2 M_2}{n_1 M_1 + n_2 M_2} = \frac{X_1}{100}\rho_1 + \frac{X_2}{100}\rho_2 \tag{7}$$

$$\sigma = \frac{\sigma_1 n_1 M_1 + \sigma_2 n_2 M_2}{n_1 M_1 + n_2 M_2} = \frac{X_1}{100}\sigma_1 + \frac{X_2}{100_2}\sigma_2, \tag{8}$$

where ρ_1 and ρ_2 are the densities of pure water and gluratic acid, and σ_1 and σ_2 are the surface tensions of pure water and glutaric acid. Hence the density ρ and surface tension σ of the cluster are related to those of the pure components 1 and 2 through weight percentages. Thus

$$\frac{d\rho}{dX_1} = (\rho_1 - \rho_2)/100, \frac{d\rho}{dX_2} = (\rho_2 - \rho_1)/100. \tag{9}$$

We also make the approximation that

$$\frac{3}{4}\pi r^3 = n_1 V_1 + n_2 V_2, \tag{10}$$

where V_i is the volume of one molecule of component i, $V_i = M_i/\rho_i$.

Plugging (2), (6)-(10) into (5), we get the following two simultaneous equations:

$$\ln\left(\frac{RH}{a_1}\right) = \frac{2}{kT}M_1\left[\frac{M_1 n_1 \sigma_1 + M_2 n_2 \sigma_2}{M_1 n_1 \rho_1 + M_2 n_2 \rho_2}\right]\left[\frac{3}{4\pi}(V_1 n_1 + V_2 n_2)\right]^{-\frac{1}{3}}$$
$$\left[1 - \frac{(\rho_1 - \rho_2)M_2 n_2}{M_1 n_1 \rho_1 + M_2 n_2 \rho_2}\right] \tag{11}$$

$$\ln\left(\frac{P_2}{P_2^{\infty}}\right) = \frac{2}{kT}M_2\left[\frac{M_1 n_1 \sigma_1 + M_2 n_2 \sigma_2}{M_1 n_1 \rho_1 + M_2 n_2 \rho_2}\right]$$
$$\left[\frac{3}{4\pi}(V_1 n_1 + V_2 n_2)\right]^{-\frac{1}{3}}\left[1 - \frac{(\rho_2 - \rho_1)M_1 n_1}{M_1 n_1 \rho_1 + M_2 n_2 \rho_2}\right]. \tag{12}$$

Since the interfacial mass transfer of GA and its aqueous-phase diffusion are expected to be sufficiently rapid, it is reasonable to assume that the concentration of GA inside the droplet is uniform and satisfies at any moment the Henry's law equilibrium; in mathematical terms, we have

$$P_2^{\infty}K_h = a_2', \tag{13}$$

where K_h is the Henry's law constant for glutaric acid. We use $K_h = 2E+8$ M/atm (R. Sander, Compilation of Henry's law constants for inorganic and organic species of potential importance in environmental chemistry, 1999, available at http://www.mpch-mainz.mpg.de/~sander/res/henry.html#2). The parameter a_2' is the activity of GA (in molarity) in the binary solution.

At this point, as long as a_1 and a_2' in equations (11) and (13) can be expressed by n_1 and n_2, we can numerically solve these two equations simultaneously for (n_1, n_2) at any given temperature T, relative humidity RH, and ambient GA vapor pressure P_2. It will then be straightforward to calculate the rate of nucleation of the GA-H_2O binary system using equation (3).

Davies and Thomas [1956] did some isopiestic studies of aqueous dicarboxylic acid solutions. Using sulfuric acid as standards, the solvent vapor pressure lowering and activities of both solvent (water) and solute (dicarboxylic acids) are determined, as shown in Table 8. From the experimental data m, ΔP, and a_2'/m provided by Davies and Thomas, it is easy to calculate the activities of water and GA in binary solutions of different concentrations (in the first column). We can then write a_1 and a_2' as a function of GA concentration from these data:

$$a_1 = -0.0097 m + 0.994; \tag{14}$$

$$a_2' = 0.8107 \ln(m) + 1.0419. \tag{15}$$

Since we have $m = (1000 n_2/(N_{av} n_1 M_1))$ where N_{av} is the Avogadro constant and, in the range of concentrations studied,

Table 8. Determining Activities of Water and GA in Glutaric Acid-Water Solution (25°C)[a]

m, mol kg⁻¹	ΔP, mm Hg⁻¹	P_1, mm Hg⁻¹	a_2'/m	a_1 (H₂O, in Mole Fraction)	a_2' (GA, in Molality)
0.493	0.199	23.581	1.142	0.992	0.563
1.092	0.422	23.358	0.977	0.982	1.067
1.416	0.480	23.300	0.904	0.980	1.280
2.186	0.680	23.100	0.755	0.971	1.650
2.403	0.725	23.055	0.723	0.970	1.737
2.880	0.806	22.974	0.649	0.966	1.869
3.789	0.996	22.784	0.567	0.958	2.148
4.114	1.080	22.700	0.552	0.955	2.271

[a]Here m is molality of GA in water solution; ΔP is lowering of water vapor pressure due to GA in the solution; P_1 is water vapor pressure over the surface of GA-H₂O solution; a_1 is activity of water in GA-H₂O binary solution; a_2' is activity of GA in GA-H₂O binary solution; a_2' here (in molality) is different from but related to the GA activity (in mole fraction) defined by equation (2).

the density of the binary solution is about 1 kg/L, we then combine (11), (12), (13) with (14) and (15) and get (16) and (17) as written below:

$$\ln\left(\frac{RH}{-0.0097\left(\frac{1000 n_2}{N_{av} n_1 M_1}\right) + 0.994}\right) = \frac{2}{kT} M_1 \left[\frac{M_1 n_1 \sigma_1 + M_2 n_2 \sigma_2}{M_1 n_1 \rho_1 + M_2 n_2 \rho_2}\right]$$

$$\left[\frac{3}{4\pi}(V_1 n_1 + V_2 n_2)\right]^{-\frac{1}{3}} \left[1 - \frac{(\rho_1 - \rho_2) M_2 n_2}{M_1 n_1 \rho_1 + M_2 n_2 \rho_2}\right] \quad (16)$$

$$\ln\left(\frac{P_2 K_h}{0.8107 \ln\left(\frac{1000 n_2}{N_{av} n_1 M_1}\right) + 1.0419}\right) = \frac{2}{kT} M_2 \left[\frac{M_1 n_1 \sigma_1 + M_2 n_2 \sigma_2}{M_1 n_1 \rho_1 + M_2 n_2 \rho_2}\right]$$

$$\left[\frac{3}{4\pi}(V_1 n_1 + V_2 n_2)\right]^{-\frac{1}{3}} \left[1 - \frac{(\rho_2 - \rho_1) M_1 n_1}{M_1 n_1 \rho_1 + M_2 n_2 \rho_2}\right]. \quad (17)$$

Now to solve for these two equations (16) and (17) at different P_2, we just need to finalize some thermodynamic data. We take ρ_1, ρ_2, σ_1 from *Lide* [1991]. For the surface tension of pure GA, σ_2, we extrapolate the data of surface tension as a function of GA concentration from *Schulman* [1995] to the pure glutaric acid and use the value of 44.60E-3 N/m.

We will first compare the model output with the nucleation rate observed by the particle counters in the case of October 10, 1998, where $T = 299.84$ K and RH = 65.7%. The model output (Table 9) shows the particle nucleation rate as a function of the mixing ratio of GA vapor in the chamber. It is shown in Table 6 that the nucleation rate was about 81.5 cm⁻³ s⁻¹ in the October 10 case. According to Table 9, for GA-H₂O system to achieve such a nucleation rate, the GA mixing ratio would have had to reach at least 800 ppb. However, considering only 50 ppbv cyclopentene was injected into the chamber initially, the [GA]_g was obviously far lower than 800 ppbv. In fact, if the yield of GA in the aerosol were any indication

(0.17%, Table 2), the GA mixing ratio was probably lower than even 1 ppb. Our model output indicates under such a condition, the GA-H₂O nucleation rate would have been less than 1E-100 cm⁻³ s⁻¹. Clearly this means no homogeneous nucleation could have occurred if the nucleation system had been GA-H₂O. The difference between our model output and the experimental observation is so large that any modeling or instrumental errors can hardly explain it. We conclude that glutaric acid-water homogeneous nucleation was too slow to account for the observed particle nucleation rate.

Another important observation relevant to the validity of GA-H₂O nucleation is provided by RH measurements. When we change the RH from the 66% (October 10 case) to 29%

Table 9. Calculating Particle Nucleation Rate as a Function of the Glutaric Acid (GA) Vapor Mixing Ratio in the GA-H₂O Binary System

[GA]_g in the Chamber,[a] ppbv	n_1[b]	n_2[c]	r_c[d] m	ΔG,[e] J	J_n[f] cm⁻³ s⁻¹
100	297	274	2.3E09[g]	1.1E-18	1.32E-94
150	142	140	1.83E-09	6.92E-19	1.26E-51
200	90	93	1.6E-09	5.22E-19	8.84E-34
300	53	57	1.35E-09	3.77E-19	1.51E-18
400	37	42	1.22E-09	3E-19	1.88E-10
500	30	34	1.14E-09	2.64E-19	1.17E-06
600	24	28	1.06E-09	2.33E-19	2.12E-3
700	21	25	1.02E-09	2.12E-19	0.396
800	18	22	9.79E-10	1.94E-19	31.6
900	17	20	9.5E-10	1.89E-19	113
1000	15	19	9.31E-10	1.7E-19	1.34E+04
1500	11	14	8.41E-10	1.42E-19	1.43E+07
2000	8	11	7.73E-10	1.18E-19	4.63E+09
2500	7	10	7.48E-10	1.05E-19	1.37E+11

[a][GA]_g is glutaric acid vapor mixing ratio.
[b, c, d, e]ΔG is the free energy required to form a cluster (radius r) containing n_1 molecules of H₂O and n_2 molecules of GA.
[f]This notation is identical to that used in Table 4.
[g]Read 2.3E-09 as 2.3 × 10⁻⁹.

(November 10 case), the model output of nucleation rate does not change much (within 20% for each GA vapor pressure). This is contrary to what we observed from particle counters (Table 6). It is, on the other hand, well known that the H_2SO_4-H_2O nucleation rate is strongly affected by water vapor partial pressure. This again supports our contention that the nucleation observed in the chamber was not GA-H_2O, but H_2SO_4-H_2O.

Because of the lack of some thermodynamic data (mainly activity, surface tension) for the products in cyclohexene-ozone and α-pinene-ozone systems, we have not been able to calculate other (organic product-water) nucleation rates with our model. However, considering the saturation vapor pressure (1.46E-10 atm) and Henry's law constant (2E8 M/atm) for adipic acid, a major product of the cyclohexene-ozone system, it is unlikely that (adipic acid-water) binary nucleation would have been fast enough to account for the observed new particle formation. Other aerosol components, including dialdehydes and ω-oxo carboxylic acids, have even higher saturation vapor pressures which makes them even less likely to participate in homogeneous nucleation. Two points are worth reiterating here. First, even though we have only identified a fraction of the aerosol organic matter in these hydrocarbon-ozone systems, mechanistic considerations suggest diacids should be the least volatile among all the products [*Seinfeld and Pandis*, 1998; *Koch et al.*, 2000]. Second, as we mentioned earlier in section 3.6, NH_3 is not expected to enhance the nucleating abilities of these oxidation products due to their weak acidity.

4.2. H_2SO_4-H_2O Particle Nucleation in the Cycloolefin-Ozone System

We use an integral nucleation model [*Hegg et al.*, 1992; *Kreidenweis and Seinfeld*, 1988] to simulate the H_2SO_4-H_2O particle nucleation and growth under the conditions in our cycloolefin-ozone experiments and compare with the observed particle production. In such a model the extent of nucleation can be predicted on the basis of a handful of simple equations: a parameterized nucleation rate as a function of RH, T, and

H_2SO_4 partial pressure, a H_2SO_4 source term (via SO_2 oxidation), a condensational sink term for H_2SO_4 condensing onto preexisting particle surface, and conservation equations for particle number and mass, and H_2SO_4 and SO_2 concentrations. Considering NH_3 was likely present in the chamber that could enhance the homogeneous nucleation rate J_n, we use a ternary nucleation model for the H_2SO_4-H_2O-NH_3 system to calculate J_n [*Coffman and Hegg*, 1995]. For this model to be applicable we set $[NH_3] = 1.3$ pptv which is probably at the lower end of the concentration range in the chamber. The integral model requires specifications of initial values of SO_2, $\cdot OH$, H_2O, T, and particle number concentration. In the case of October 10 the number concentration of preexisting particles was about 80 cm^{-3}, given by the TSI 3025A counter. We take $[SO_2]_0 = 100$ pptv as the initial value for our calculation, according to the SO_2 analyzer. Both H_2SO_4 and hydroxyl were detected by the chemical ionization mass spectrometer. We also take the lower-end values, $[H_2SO_4]_0 = 2$ pptv and $[\cdot OH]_0 = 5E+6$ molecules/cm^3, as the model inputs. Our model results have proven rather insensitive to the initial H_2SO_4 vapor concentration. Figure 1 shows the model output of particle number concentration as a function of time compared with that observed by the TSI3025A particle counter.

The model output simulates the new particle production very well until about 5 min after the onset of nucleation (1327 LT), when the actual particle concentration started to level off, whereas the model still predicted a rapid "burst" of new particles. When we ran the model to simulate another case of cyclopentene-ozone particle production but with 1 ppbv SO_2 initially in the chamber, we saw similar results: The model output could well simulate the particle production in the first 5 min or so, but soon after that, the actual particle number concentration leveled off, while the model predicted more particle production. Furthermore, the particle sizes predicted by the integral model alone were too small to explain the sizes observed by the DMA in the chamber experiments.

These "inconsistencies" between the model outputs and the observations can actually be easily interpreted by our earlier
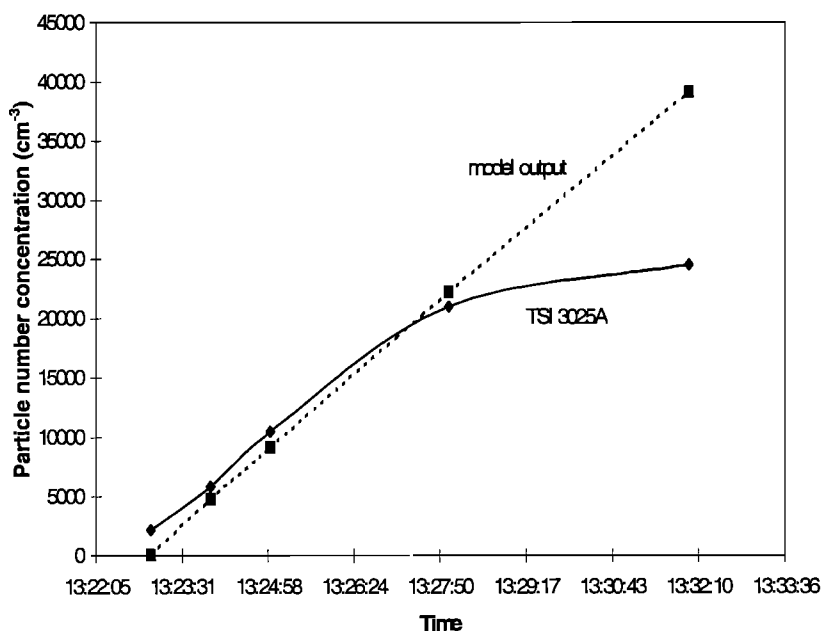

Figure 1. TSI 3025A and model output of new particle formation in the case of October 10, 1998.

proposals. As soon as the H_2SO_4-H_2O nuclei were formed, organic products continuously produced in the reaction system would partition into these nuclei, initiate substantial water condensation and quickly increase the nuclei surface area. At some point (about 5 min after nucleation onset in the October 10 case), H_2SO_4 vapor molecules would start to primarily condense on these large surfaces rather than nucleate new particles, therefore effectively killing off further nucleation. As a result, far fewer particles than the model's prediction would be formed, and they would grow into much larger sizes. In comparison, on October 13 when only SO_2 and ozone were initially present in the chamber (Table 4), the particle number concentration grew up to over 100,000 cm^{-3} within 10 min. Since there were not enough organic species produced, neither partitioning of organics nor water condensation occurred substantially to grow the newly formed H_2SO_4-H_2O nuclei, resulting in only very small particles ($R_m \sim 5$ nm) even after 40 min of observation.

4.3. Partitioning of Glutaric Acid Into the Fresh H_2SO_4-H_2O Nuclei

It is well known that besides glutaric acid (GA), other oxidation products in the cyclopentene-ozone system will also partition into the aerosol phase, for example, glutaldehyde and 5-oxo-pentanoic acid [Hatakeyama et al., 1987]. However, as we have mentioned earlier, GA is expected to be one of the major aerosol products under ambient conditions. Therefore, instead of trying to model the partitioning processes for all the products, we choose to develop a simple diagnostic model to study the partitioning of the major product, GA, into the H_2SO_4-H_2O nuclei. Another reason for doing this is that GA has the highest solubility among all the known particulate products from cyclopentene ozonolysis. Our model results can then be compared with the mass concentration of particulate GA obtained from filter sampling of aerosol and subsequent IC analyses. Other oxidation products can be incorporated into this model later if found necessary.

It is worth noting that our approach throughout this exercise is at least semi-empirical, i.e., wherever possible we utilize the observational data to constrain and simplify our calculations. For example, the most straightforward methodology for calculating the amount of GA in the aerosol would simply be to assume that all of the GA was instantaneously produced in the gas phase through ozonolysis of cyclopentene. The GA then partitioned into the aerosol droplets with the observed asymptotic volume (~9.8 $\mu m^3/cm^3$ in the October 10 case, after the hygroscopic correction for the DMA measurement), assuming Henry's law equilibrium. In this scenario one gets a GA mass concentration in the condensed phase of 0.59 $\mu g/m^3$, somewhat higher than the measured value of 0.41 $\mu g/m^3$ from the IC analyses (uncertainty: ±20%). However, one should realize this scenario assumes no kinetic limitations to the interphase transfer and further assumes that the GA Henry's law constant for the bulk solution is exactly applicable to the actual aerosol droplets in the chamber. While the latter assumption is difficult to completely avoid in even diagnostic studies, the former can be tested with the following diagnostic box model.

As in other time-dependent box models [e.g., Chameides, 1984], our model treats the gas-phase chemistry as well as the partitioning of GA vapor into the aqueous-phase aerosol. The aqueous-phase chemistry is worth exploring in the future but

neglected here as, in this study, we assume all the oxidation processes take place in the gas phase. Our purpose is to evaluate whether such an assumption could be viable to explain our observations. In the gas phase,

$$\frac{dX}{dt} = k[\text{cyclopentene}][\text{ozone}]\gamma - \Phi_c, \qquad (18)$$

where k is the reaction rate constant (6.3E-16 cm^3 molecule^{-1} s^{-1}), X is the gas-phase concentration of GA (cm^{-3}) in the chamber, [cyclopentene], [ozone] are the respective gas-phase concentrations (cm^{-3}), γ is the yield of GA in the gas phase, and Φ_c is the interphase flux rate of GA vapor into aerosols ($cm^{-3}s^{-1}$). The coagulation and wall loss can be to the first order ignored according to our calculations.

Using the Fuchs and Sutugin [1970] equation, we have

$$\Phi_c = 4\pi R_p \alpha D_g \beta N_p (X - X_s), \qquad (19)$$

where α corrects for using the mean radius R_p in the condensation rate equation [Okuyama et al., 1988], D_g is the diffusivity of GA molecules (taken as 0.078 cm^2 s^{-1}), β is a correction factor which extends the condensation equation through the transition and kinetic regimes [Dahneke, 1983], N_p is the aerosol number concentration (cm^{-3}), and X_s is the GA vapor concentration at the particle surface (cm^{-3}).

Assuming the molar concentration of GA in the aerosol droplets is Y (mol/L), we can apply Henry's law:

$$(X_s / N_{av})RTK_h' = Y, \qquad (20)$$

where N_{av} is Avogadro's constant and K_h' is the effective Henry's law constant.

In the aqueous-phase we assume the flux of GA vapor is fully scavenged by these aerosol droplets with a mean volume density V_p ($\mu m^3/cm^3$ air). We then have the mass balance equation for GA in the aqueous phase

$$\frac{dY}{dt} = \Phi_c /(N_{av}V_p). \qquad (21)$$

Here we assume all droplets are homogeneously mixed. Since the mixing time in a micron-sized droplet is about 0.01 s [Schwartz and Freiberg, 1981] and we are interested in temporal variations on the timescale of minutes, this approximation is appropriate. At this point, by combining (18), (19), (20), and (21), we shall be able to solve these coupled equations numerically for X and Y as long as α, β, γ, K_h', N_p, V_p, R_p are known.

The values of α, β are readily available or calculable from Okuyama et al. [1988], Lide [1991], and Seinfeld and Pandis [1998]. Hatakeyama et al. [1984] determined nicely that the collisionally stabilized Criegee intermediate from the cyclopentene-ozone reaction has a yield of 5.2%. Such a stabilized intermediate would mechanistically only lead to 5-oxo-pentanoic acid and glutaric acid. The yield of 5-oxo-pentanoic acid is estimated to be 1% [Hatakeyama et al., 1987]. Therefore we take 4.2% as the yield of gas-phase GA (γ). In the droplets composed of H_2SO_4 and H_2O as a result of homogeneous nucleation, the pH value is found to be lower than 1.0. At such a low pH the effective Henry's law constant K_h' of GA is essentially the same as the Henry's law constant
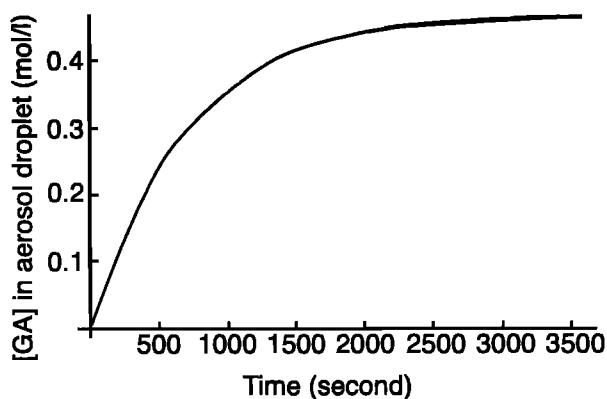
Figure 2. GA molar concentration in the aerosol, [GA], during particle growth process in the case of October 10, 1998. Note that due to the use of a constant aerosol volume density V_p when solving the equations, this actually better reflects the time dependence of the GA mass concentration in the chamber, rather than the actual molar concentration in the aerosol droplets. One can recover the mass concentration by multiplying the given concentration by the corresponding V_p.

K_h (2E+8 M/atm). We note it is uncertain whether the Henry's law constant in the bulk solution is exactly applicable to tiny aerosol droplets, and this uncertainty is further compounded by the chemical complexities of these droplets that could include H_2SO_4 and other organic species. Since these uncertainties are currently intractable, we here simply adopt the bulk data for our diagnostic purpose.

A key facet of this assessment is the GA vapor concentration above the aerosol droplets (X_s) that will largely determine the rate of GA interphase transfer. This is estimated from Henry's law and the instantaneous GA concentration in the aerosol droplets (Y), as implied by equation (20). Estimation of the aqueous concentration of GA itself, calculated by equation (21), utilizes observed value of the aerosol volume density V_p. This utilization of observed V_p avoids the difficult problem of calculating the water condensation onto the complex H_2O-H_2SO_4-GA (and likely other organic species) solution drops in which their activities are largely unknown. Indeed, our calculations suggest this approach can lead to even further simplifications as described below.

While N_p, V_p, R_p are all evolving during this process, the model results for the asymptotic values of X and Y turn out to be very insensitive to the different sets of (N_p, V_p, R_p) values being used. Particularly, the GA molar concentration in the aerosol (Y) near the end of phase partitioning is found to have little dependence upon (N_p, V_p, R_p) values, consistent with theoretical predictions that will be seen from equation (22). Thus, rather than writing out detailed time-dependent equations for these variables (essentially parameterizations based on observed values), we input a certain set of (R_p, N_p, V_p) values (e.g., at $t = 5$ min) for which the model should yield good enough results for our purpose (comparing with filter/IC results). However, because of this, one must be careful in interpreting the results. For example, the time dependence of Y, which ostensibly shows the time variance of the GA molar concentration in the aerosol droplets (mol/L), actually rather represents the time variance of the GA mass concentration in the chamber (μg/m^3).

In the case of October 10, 1998, the measurements show the cyclopentene and ozone mixing ratios as a function of time as follows: [cyclopentene] = 56.6 exp[-0.001 t] ppbv; [ozone] = 93.0 exp[-0.0005 t] ppbv; plus, we take N_p = 7520 cm^{-3}, R_p = 0.02 μm, V_p = 0.55 μm^3/cm^3 at $t = 5$ min as input values. Plug these into (18)-(21) and solve for Y. We plot Y as a function of time in Figure 2.

When other sets of (N_p, R_p, V_p) values (e.g., $t = 0$, 10 min, 20 min) are used as model inputs, the results of GA molar concentration in the aerosol (Y) and vapor concentration (X) show little variation from Figure 2. Such insensitivity to (N_p, R_p, V_p) values is rather surprising at first sight. However, we see the final molar concentration of GA in the aerosol is about 0.46 M, equivalent to 6 g GA/100 g water. This is far lower than the concentration in a saturated GA solution (solubility of GA equal to 116 g/100 g water) [Saxena and Hildemann, 1996]. Thus, the partitioning process here is essentially a process of continuously produced GA quickly dissolving into the aerosol droplets. Water vapor would then also continuously condense onto the droplets to compensate for the lowering of water activity (and thus water vapor concentration at the surface), due to the dissolution of GA and likely other organic products. Since the GA solution was never saturated, the final GA concentration in the aerosol turned out to be mainly modulated by its gas-phase production, which was well measured and modeled. The chemically produced GA vapor would continuously dissolve into the aerosol droplets until the equilibrium between the gas and aqueous phase was established (i.e., when the gas-to-particle flux became zero).

Our model outputs show the GA molar concentration (Y) in the aerosol increases asymptotically (Figure 2), although the slope at the beginning should in fact be steeper due to the use of a constant volume V_p. However, once again, for the reasons we have just stated, the uncertainty of the model outputs of [GA] near the end of phase partitioning (the asymptotic value in Figure 2), caused by using a constant set of (N_p, R_p, V_p), is expected to be small. At least such an uncertainty should be smaller than the measurement uncertainties of N_p, R_p, V_p, and gas concentrations.

An aerosol sample was collected between t_1 = 1020 s and t_2 = 3420 s in the above case. Figure 2 shows the molar concentrations of GA in the aerosol (Y) at t_1 and t_2 are 0.36 and 0.46 mol/L, respectively. The DMA-derived aerosol volume densities V_p, after hygroscopic corrections, are 4.30 and 5.34 μm^3/cm^3, respectively. Calculations then show the mass concentration of GA in the chamber, during this time interval, has an average value of 0.48 μg/m^3 air. This is in quite good agreement with that identified by IC (0.41 μg/m^3), considering the overall uncertainty of the IC analyses is about 20%. However, both values are somewhat lower than that predicted by calculations simply using partitioning equilibrium (0.59 μg/m^3), as shown earlier. This implies that there could be some kinetic limitations to the interphase mass transfer during such an aerosol growth process, where chemical reaction and phase partitioning of certain products take place simultaneously. It should be pointed out that, under some circumstances, the actual gas/aerosol partitioning mechanism can be much more complicated than what is described here, as it is determined by both the partitioning species and the phases they can partition into. For example, a widely proposed mechanism is based upon the partitioning of organic species between the gas phase and the organic material phase

in the aerosol [*Pankow*, 1994a, 1994b; *Odum et al.*, 1996]. In our model the partitioning is between the gas phase and the aerosol aqueous phase. It seems reasonable to adopt the latter mechanism for a compound as soluble as glutaric acid, while for less polar (thus perhaps more hydrophobic) products such as those from the oxidation of aromatics and α-pinene [*Odum et al.*, 1996], the first mechanism could be more suitable. Indeed, secondary organic compounds may exist in all three phases: the gas, the organic aerosol material, and the aqueous phase, at least for high relative humidities [*Saxena et al.*, 1995]. It is our view that the mechanism suggested by Pankow (and others) and that suggested here by ourselves constitute two rather extreme cases in a "continuous" spectrum of the actual phase partitioning mechanism.

In several other cases the model outputs of GA mass in aerosol are also in good agreement with those from the filters. In fact, if we solve the above equations (18)-(21) in symbolic terms, the final GA molar concentration in the aerosol, [GA]$^\infty$, can be written as follows:

$$[GA]^\infty = \frac{A[\text{ozone}]_o[\text{cyclopentene}]_o\gamma}{N_{av}\left[\dfrac{0.1013}{K_h' RT}\right]}, \quad (22)$$

where A is related to the ozone and cyclopentene reaction constant and decay rate, $[\text{ozone}]_o$ and $[\text{cyclopentene}]_o$ are initial gas-phase concentrations, and K_h' is the effective Henry's law constant for GA. While the approximations utilized in its derivation render this an approximate and by no means general solution, we feel it will have considerable prognostic power for scenarios similar to that treated here. On the basis of (22) we present two theoretical predictions and their experimental support:

1. When the initial concentrations of O_3 and cyclopentene are elevated, the equilibrium molar concentration of GA in the aerosol should also rise. The molar yield of GA in the aerosol, as seen from $[GA]^\infty/[\text{cyclopeneten}]_o$, is also expected to increase as the initial ozone level increases. This could quantitatively explain why the molar yields reported by *Hatakeyama et al.* [1985, 1987] are higher than in ours, as has been qualitatively suggested in some earlier work [e.g., *Satsumabayashi et al.*, 1990].

2. The pH of the fresh nuclei could play an important role in affecting the partitioning of organic compounds into them. For a diprotic acid like a dicarboxylic acid the effective Henry's law constant K_h' is

$$K_h' = K_h\left(1 + \frac{K_a^1}{[H^+]} + \frac{K_a^1 K_a^2}{[H^+]^2}\right), \quad (23)$$

where K_h is the Henry's law constant, and K_a^1 and K_a^2 are the first and second step dissociation constants of the acid. When the $[H^+]$ of the fresh nuclei is high (such as in the H_2SO_4-H_2O nuclei), strong acids with high K_a^1 and K_a^2 would increase the K_h' effectively according to (23). Then equation (22), which should be applicable to other secondary aerosol components, predicts that the concentrations of these acids in the aerosol at the end of phase partitioning would become higher. Under conditions in the MBL where the NH_3 mixing ratio is sufficiently low thus rendering H_2SO_4-H_2O binary nucleation

the dominant nucleation process, the pH of the freshly formed nuclei could be as low as 1. Then, as shown above, the acids with pK_a^1 close to 1 are expected to be the major partitioning species, for example, oxalic acid ($pK_a^1 = 1.23$) and malonic acid ($pK_a^1 = 2.83$). In comparison, succinic acid ($pK_a^1 = 4.16$), glutaric acid ($pK_a^1 = 4.31$), or adipic acid ($pK_a^1 = 4.43$) should contribute much less to the aerosol mass, provided all of these acids are present in comparable amounts. Such a theoretical prediction finds support from several field measurements of dicarboxylic acids in remote marine and urban aerosols [e.g., *Kawamura and Sakaguchi*, 1999; *Kawamura and Ikushima*, 1993]. Since C2 and C3 diacids could be final oxidation products from longer-chain acids, such a preferential partitioning into the condensed phase would further enhance their concentrations in the submicron aerosols.

5. Conclusions and Some Applications to the MBL

A series of controlled experiments were carried out in the Calspan Corporation's 600 m^3 environmental chamber where some secondary organic aerosol formation processes were simulated and studied. Since the concentrations of the precursors and oxidants used, and the chamber conditions (*T, P*, RH, etc.), were much closer to the values expected in certain MBL regions than have previously been examined, many results in these experiments could be more plausibly applied to the MBL.

1. The three precursor-ozone systems studied, with no seed aerosol present, readily formed new submicron aerosols at very low reactant levels.

2. Identification of water-soluble compounds in the formed aerosols showed agreement with some previous studies. However, the yields of organic products in the Calspan experiments were lower, probably due to the lower concentrations of initial reactants.

3. A three-step procedure is proposed to explain the observed particle nucleation: hydroxyl production → H_2SO_4 formation → H_2SO_4-H_2O (perhaps together with NH_3) homogeneous nucleation. We also propose that certain secondary organic products would not make an important contribution to new particle nucleation but, rather, they would partition into the H_2SO_4-H_2O fresh nuclei, enhance water condensation, and help grow these nuclei into a larger size range. Such a scheme is plausible in the MBL where trace amounts of SO_2, NH_3, O_3, and background hydrocarbons are ubiquitous and preexisting particles are relatively few. It also provides a viable mechanism to explain why sulfate and organics have often been found present in a single aerosol particle.

4. The well-known source of cyclopentene or cyclohexene is from urban pollution, e.g., automobile exhaust. Assuming an ozone level of 20 ppb, the lifetime of cyclopenetene due to ozone oxidation is about 1 hour. Therefore the cycloolefins, emitted in many urban coastal regions, can be transported into the marine atmosphere under certain meteorological conditions. During such transport, oxidation to dicarboxylic acids and other products could take place, and they could partition into preexisting particles through the mechanism proposed above. However, if the ozone level were higher or the wind speed were significantly slower, the above chemical and particle formation processes would mostly take place within the coastal region. Dicarboxylic acids could then still be transported to the MBL in the aerosols they have partitioned into.

On the other hand, if cycloolefins have a significant marine source and their oxidation products can provide sufficient mass flux, then our proposed mechanism could be a more widespread pathway to form secondary organic aerosols in the MBL. We further note that such a pathway can be applicable to primary hydrocarbon precursors of dicarboxylic acids other than cycloolefins (as much as 50% of the carbon mass emitted from the ocean surface could be in the form of olefins [cf. *Bonsang et al.*, 1991]), as well as secondary organic species produced in the marine atmosphere which have similar properties as the ones studied here.

5. H_2SO_4 is a superb nucleating species, while secondary organic compounds (certainly with possible exceptions, e.g., certain α-pinene oxidation products) play a role more confined to growing newly formed particles. In the MBL such a scheme of particle nucleation (H_2SO_4-H_2O-NH_3) followed by particle growth (through dissolution of organic compounds and condensation of water vapor) would allow particles to grow into the CCN size range reasonably fast and therefore help reconcile calculated nucleation and growth rates with the observed CCN budget. Different proposals have emerged as to the detailed mechanism of particle growth within such a scheme [e.g., *Kreidenweis and Seinfeld*, 1988; *Kulmala et al.*, 2000]. Indeed, this variety might very well be necessary to adequately treat the different suites of organic and inorganic species that range widely in their solubilities, volatilities, and other properties. Nevertheless, it appears that the traditional treatment of only H_2SO_4 particle nucleation and growth should be revised to include selected organic compounds as important factors in the particle growth process [*Lin et al.*, 1992; *Raes and Van Dingenen*, 1992]. Finally, it is to be kept in mind that besides the one discussed above, there is another potential route of CCN formation, i.e., new particle production (via H_2SO_4-H_2O nucleation) in the free troposphere followed by growth and subsidence into the MBL [e.g., *Raes*, 1995]. A number of field measurements seem to support such an aerosol entrainment process [*Clarke et al.*, 1996, 1998]. However, further discussion on which of the two schemes contributes most to the aerosol and CCN concentrations in the MBL, or how the two processes compete, is beyond the scope of this work.

References

Atkinson, R., Gas-phase tropospheric chemistry of organic compounds, *J. Phys. Chem. Ref. Data Monogr.*, 2, 1-216, 1994.

Bonsang, B., D. Martin, G. Lambert, M. Kanakidou, J. C. Le Roulley, and G. Sennequier, Vertical distribution of nonmethane hydrocarbons in the remote marine boundary layer, *J. Geophys. Res.*, 96, 7313-7324, 1991.

Chameides, W. L., The photochemistry of a remote marine stratiform cloud, *J. Geophys. Res.*, 89, 4739-4755, 1984.

Chow, J. C., J. G. Watson, E. M. Fujita, Z. Q. Lu, D. R. Lawson, and L. L. Ashbaugh, Temporal and spatial variations of PM2.5 and PM10 aerosol in Southern California Air Quality Study, *Atmos. Environ.*, 28, 2061-2080, 1994.

Clarke, A. D., Z. Li, and M. Litchy, Aerosol dynamics in the equatorial

Pacific marine boundary layer: Microphysics, diurnal cycles and entrainment, *Geophys. Res. Lett.*, 23, 733-736, 1996.

Clarke, A. D., J. L. Varner, F. Eisele, R. L. Mauldin, D. Tanner, and M. Litchy, Particle production in the remote marine atmosphere: Cloud outflow and subsidence during ACE 1, *J. Geophys. Res.*, 103, 16,397-16,409, 1998.

Coffman, D. J., and D. A. Hegg, A preliminary study of the effect of ammonia on particle nucleation in the marine boundary layer, *J. Geophys. Res.*, 100, 7147-7160, 1995.

Corrigan, C. E., and T. Novakov, Cloud condensation nuclei activity of organic compounds: A laboratory study, *Atmos. Environ.*, 33, 2661-2668, 1999.

Cruz, C. N., and S. N. Pandis, A study of the ability of pure secondary organic aerosol to act as cloud condensation nuclei, *Atmos. Environ.*, 31, 2205-2214, 1997.

Cruz, C. N., and S. N. Pandis, The effect of organic coatings on the cloud condensation nuclei activation of inorganic atmospheric aerosol, *J. Geophys. Res.*, 103, 13,111-13,123, 1998.

Dahneke, B., Simple kinetic theory of Brownian diffusion in vapors and aerosols, in *Theory of Dispersed Multiphase Flow*, pp. 97-133, Academic, San Diego, Calif., 1983.

Davies, M., and D. K. Thomas, Isopiestic studies of aqueous dicarboxylic acid solutions, *J. Phys. Chem.*, 60, 41-44, 1956.

Dingenen, R.V., and F. Raes, Ternary nucleation of methane sulphonic acid, sulfuric acid and water vapour, *J. Aerosol Sci.*, 24, 1-17, 1993.

Fuchs, N. A., and A. G. Sutugin, *Highly Dispersed Aerosols*, Butterworth-Heinemann, Woburn, Mass., 1970.

Grosjean, D., K. V. Cauwenberghe, J. P. Schmid, P E. Kelley, and J. N. Pitts Jr., Identification of C_3-C_{10} aliphatic dicarboxylic acids in airborne particulate matter, *Environ. Sci. Technol.*, 12, 313-317, 1978.

Guenther, A., et al., A global model of natural volatile organic compound emissions, *J. Geophys. Res.*, 100, 8873-8892, 1995.

Harrington, D. Y., and S. M. Kreidenweis, Simulation of sulfate aerosol dynamics, I, Model description, *Atmos. Environ.*, 32, 1691-1700, 1998.

Hatakeyama, S , H. Kobayashi, and H. Akimoto, Gas-phase oxidation of SO_2 in the ozone-olefin reactions, *J. Phys. Chem.*, 88, 4736-4739, 1984.

Hatakeyama, S., T. Tanonaka, J. Weng, H. Bandow, H. Takagi, and H. Akimoto, Ozone-cyclohexene reaction in air: Quantitative analysis of particulate products and the reaction mechanism, *Environ. Sci. Technol.*, 19, 935-942, 1985.

Hatakeyama, S., M. Ohno, J. Weng, H. Takagi, and H Akimoto, Mechanism for the formation of gaseous and particulate products from ozone-cycloalkene reactions in air, *Environ. Sci. Technol.*, 21, 52-57, 1987.

Hatakeyama, S., K. Izumi, T. Fukuyama, and H. Akimoto, Reactions of ozone with α-pinene and β-pinene in air: Yields of gaseous and particulate products, *J. Geophys. Res.*, 94, 13,013-13,024, 1989.

Hegg, D., D Covert, and V. Kapustin, Modeling a case of particle nucleation in the marine boundary layer, *J. Geophys. Res.*, 97, 9851-9857, 1992.

Hoffmann, T., J. Odum, F. Bowman, D. Collins, D. Klockow, R. Flagan, and J. Seinfeld, Formation of organic aerosols from the oxidation of biogenic hydrocarbons, *J. Atmos. Chem.*, 26, 189-222, 1997.

Hoffmann, T., R. Bandur, U. Marggraf, and M. Linscheid, Molecular composition of organic aerosols formed in the α-pinene/O_3 reaction: Implications for new particle formation processes, *J. Geophys. Res.*, 103, 25,569-25,578, 1998.

Hoppel, W., G. Frick, P. Caffrey, L. Pasternack, T. Albrechcinski, J. Ambrusko, W. Sullivan, D. Hegg, and S. Gao, Report on the characterization of Calspan's 600 m^3 chamber in preparation for the NOPP aerosol processes experiments, *Nav. Res. Lab. Doc. NRL/MR/6110-99-8370*, Nav. Res. Lab., Washington, D. C., 1999.

Huebert, B., and R. Charlson, Uncertainties in data on organic aerosols, *Tellus, Ser. B.*, 52, 1249-1255, 2000.

Jaecker-Voirol, A., and P. Mirabel, Heteromolecular nucleation in the sulfuric acid-water system, *Atmos. Environ.*, 23, 2053-2057, 1989.

Kalberer, M., J. Yu, D. Cocker, R. Flagan, and J. Seinfeld, Aerosol formation in the cyclohexene-ozone system, *Atmos. Environ.*, 34, 4894-4901, 2000.

Kawamura, K., and K. Ikushima, Seasonal changes in the distribution of dicarboxylic acids in the urban atmosphere, *Environ. Sci. Technol.*, 27, 2227-2235, 1993.

Kawamura, K., and F. Sakaguchi, Molecular distributions of water-

soluble dicarboxylic acids in marine aerosols over the Pacific Ocean including tropics, *J. Geophys. Res., 104*, 3501-3509, 1999.

Kawamura, K., R. Semérè, Y. Imai, Y. Fujii, and M. Hayashi, Water-soluble dicarboxylic acids and related compounds in Antarctic aerosols, *J. Geophys. Res., 101*, 18,721-18,728, 1996.

Kiang, C. S., D. Stauffer, V. A. Mohnen, and J. Bricard, Heteromolecular nucleation theory applied to gas-to-particle conversion, *Atmos. Environ., 7*, 1279-1283, 1973.

Koch, S., R. Winterhalter, E. Uherek, A. Kolloff, P. Neeb, and G. Moortgat, Formation of new particles in the gas-phase ozonolysis of monoterpenes, *Atmos. Environ., 34*, 4031-4042, 2000.

Korhonen, P., M. Kulmala, A. Laaksonen, Y. Viisanen, R. McGraw, and J. H. Seinfeld, Ternary nucleation of H_2SO_4, NH_3, and H_2O in the atmosphere, *J. Geophys. Res., 104*, 26,349-26,353, 1999.

Kreidenweis, S., and J. Seinfeld, Nucleation of sulfuric acid-water and methanesulfonic acid-water solution particles: Implications for the atmospheric chemistry of organosulfur species, *Atmos. Environ., 22*, 283-296, 1988.

Kulmala, M., L. Pirjola, and J. Makela, Stable sulfate clusters as a source of new atmospheric particles, *Nature, 404*, 66-69, 2000.

Lide, R. D., *Handbook of Chemistry and Physics*, 72nd ed., CRC Press, Boca Raton, Fla., 1991.

Lin, X., L. Chameides, C. S. Kiang, A. W. Stelson, and H. Berresheim, A model study of the formation of cloud condensation nuclei in remote marine areas, *J. Geophys. Res., 97*, 18,161-18,171, 1992.

Matsumoto, K., H. Tanaka, I. Nagao, and Y. Ishizaka, Contribution of particulate sulfate and organic carbon to cloud condensation nuclei in the marine atmosphere, *Geophys. Res. Lett., 24*, 655-658, 1997.

Murphy, D. M., D. S. Thomson, and M. J. Mahoney, In situ measurements of organics, meteoritic material, mercury, and other elements in aerosols at 5 to 19 kilometers, *Science, 282*, 1664-1669, 1998.

Novakov, T., and J. E. Penner, Large contributions of organic aerosols to cloud-condensation-nuclei concentrations, *Nature, 365*, 823-826, 1993.

Novakov, T., D. A. Hegg, and P. V. Hobbs, Airborne measurements of carbonaceous aerosols on the East Coast of the United States, *J. Geophys. Res., 102*, 30,023-30,030, 1997.

Odum, J., T. Hoffmann, F. Bowman, D. Collins, R. Flagan, and J. H. Seinfeld, Gas/particle partitioning and secondary organic aerosol yields, *Environ. Sci. Technol., 30*, 2580-2585, 1996.

Okuyama, K., Y. Kousaka, S. Kreidenweis, R. C. Flagan, and J. H. Seinfeld, Studies in binary nucleation: The dibutylphthalate/dioctylphthalate system, *J. Chem. Phys., 89*, 6442-6453, 1988.

Pankow, J., An absorption model of gas/particle partitioning of organic compounds in the atmosphere, *Atmos. Environ., 28*, 185-188, 1994a.

Pankow, J., An absorption model of the gas/aerosol partitioning involved in the formation of secondary organic aerosol, *Atmos. Environ., 28*, 189-193, 1994b.

Raes, F., Entrainment of free tropospheric aerosols as a regulating mechanism for cloud condensation nuclei in the remote marine boundary layer, *J. Geophys. Res., 100*, 2893-2903, 1995.

Raes, F., and R. Van Dingenen, Simulations of condensation and cloud condensation nuclei from biogenic SO_2 in the remote marine boundary layer, *J. Geophys. Res., 97*, 12,901-12,912, 1992.

Renninger, R. G., F. C. Hiller, and R. C. Bone, Comment on "Self-nucleation in the sulfuric acid-water system," *J. Chem. Phys., 75*, 1584, 1981.

Satsumabayashi, H., H. Kurita, Y. Yokouchi, and H. Ueda, Photo-chemical formation of particulate dicarboxylic acids under long-range transport in central Japan, *Atmos. Environ., Part A, 24*, 1443-1450, 1990.

Saxena, P., and L. Hildemann, Water-soluble organics in atmospheric particles: A critical review of the literature and application of thermodynamics to identify candidate compounds, *J. Atmos. Chem., 24*, 57-109, 1996.

Saxena, P., L. Hildemann, P. McMurry, and J. Seinfeld, Organics alter hygroscopic behavior of atmospheric particles, *J. Geophys. Res., 100*, 18,755-18,767, 1995.

Schulman, M. L., Influence of atmospheric organic compounds on cloud microphysics, Ph.D. thesis, Univ. of Wash., Seattle, 1995.

Schwartz, S. E., and J. E. Freiberg, Mass-transport limitation to the rate of reaction of gases in liquid droplets: Application to oxidation of SO_2 in aqueous solutions, *Atmos. Environ., 15*, 1129-1144, 1981.

Seinfeld, J. H., and S. N. Pandis, *Atmospheric Chemistry and Physics*, John Wiley, New York, 1998.

Simpson, D., A. Guenther, C. N. Hewitt, and R. Steinbrecher, Biogenic emissions in Europe, 1, Estimates and uncertainties, *J. Geophys. Res., 100*, 22,875-22,890, 1995.

Stockwell, W. R., and J. G. Calvert, The mechanism of the $HO-SO_2$ reaction, *Atmos. Environ., 17*, 2231-2235, 1983.

Turpin, B.J., J.J. Huntzicker, and S.V. Hering, Investigation of organic aerosol sampling artifacts in the Los Angeles basin, *Atmos. Environ., 28*, 3061-3071, 1994.

Wilemski, G., Composition of the critical nucleus in multicomponent vapor nucleation, *J. Chem. Phys., 80*, 1370-1372, 1984.

Wolff, G.T., M. S. Ruthosky, D. P. Stroup, and P. E. Korsog, A characterization of the principal PM-10 species in Clarmont (summer) and Long Beach (fall) during SCAQS, *Atmos. Environ., Part A, 25*, 2173-2186, 1991.

Yokouchi, Y., H. J. Li, T. Machida, S. Aoki, and H. Akimoto, Isoprene in the marine boundary layer (Southeast Asian Sea, eastern Indian Ocean, and Southern Ocean): Comparison with dimethyl sulfide and bromoform, *J. Geophys. Res., 104*, 8067-8076, 1999.

Yu, J., D.R Cocker III, R. Griffin, R. Flagan, and J. Seinfeld, Gas-phase ozone oxidation of monoterpenes: Gaseous and particulate products, *J. Atmos. Chem., 34*, 207-258, 1999.

T. Albrechcinski, J. Ambrusko, and W. Sullivan, Calspan-University of Buffalo Research Center, Buffalo, NY 14225.

P. F. Caffrey, G. Frick, and L. Pasternack, Naval Research Laboratory, Washington, D. C. 20375-5000

C. Cantrell, National Center for Atmospheric Research, Boulder, CO 80307-3000.

S. Gao and D. A. Hegg (corresponding author), Department of Atmopsheric Sciences, University of Washington, Box 351640, Seattle, WA 98195-1640. (sgao@u.washington.edu; deanhegg@atmos.washington.edu)

T. W. Kirchstetter, Lawrence Berkeley National Laboratory, Berkeley, CA 94720.